Electronic Supporting Information

Carbon nanotubes-gold nanohybrid as potent electrocatalyst for oxygen reduction in alkaline media

Adina Morozan,[a,#] Simon Donck,[b,#] Vincent Artero,[a*] Edmond Gravel,[b] Eric Doris[b*]

# These authors contributed equally to this work.

[a]Laboratoire de Chimie et Biologie des Métaux, Université Grenoble Alpes, CNRS UMR 5249, CEA iRTSV, 17 rue des Martyrs, F-38000 Grenoble, France
vincent.artero@cea.fr

[b]CEA, iBiTecS, Service de Chimie Bioorganique et de Marquage, 91191 Gif-sur-Yvette, France.
eric.doris@cea.fr

Table of Content

Chemicals and materials

Chemical reagents were purchased from Sigma-Aldrich and used as received. THF (from Carlo Erba) was distilled over sodium/benzophenone prior to use. Multi-walled carbon nanotubes (CNTs) were Multi-walled carbon nanotubes (MWCNTs) were obtained from Prof. Haiyan Li (Xiamen University, China) and prepared by catalytic decomposition of methane on a Ni–Mg–O catalyst according to the previously reported method.[1] Amphiphilic nitrilotriacetic-diyne lipid (DANTA) was synthesized according to our procedure reported elsewhere.[2] Cationic poly(diallyldimethylammonium chloride) (PDADMAC), tetrahydroxymethylphosphonium chloride (THPC) and $HAuCl_4$ were obtained from Sigma-Aldrich. Nafion® 117 solution (5 wt. % in a mixture of lower aliphatic alcohols and water, Sigma-Aldrich) was used. Oxygen gas (Air Products ultrapur quality) was of 99.995% purity

Assembly of the AuCNTs nanohybrid

Self-assembly and polymerization of the amphiphile on the CNTs

DANTA (20 mg) was dissolved in 25 mM Tris aqueous buffer (2 mL, pH 8) and CNTs (50 mg) were added. The mixture was submitted to probe-sonication (5 min, 300 ms pulses per second, 25 W output power) and a stable suspension was obtained. Sonication was performed using a Branson Sonifier 450 ultrasonicating probe. After transfer into 1.5 mL Eppendorf® tubes, amorphous carbon was removed by centrifugation (5000 *×g*, 3 min). The supernatants were collected and centrifuged again (11000 *×g*, 45 min) to separate the DANTA-decorated CNTs from the excess of amphiphile. The supernatant was discarded while the pellets were resuspended in fresh Tris-buffer and centrifuged once more (11000 *×g*, 45 min). The final pellets were resuspended in buffer (1.5 mL) and submitted to UV irradiation (254 nm, 8 h) to polymerize the diacetylene groups and yield stabilized nanoring assemblies.

Assembly of the second layer on the nanoring-coated CNTs

After polymerization, the Tris-buffer volume was readjusted to 1.5 mL (to compensate the loss due to evaporation) and the suspension was stirred in the presence of PDADMAC (700 µL of a 20 % water solution) for 1 h to permit the formation of the two-layer assembly. Polymer in excess was removed by centrifugation (11000 *×g*, 30 min) and the pellets were resuspended in Tris-buffer (2 mL). This operation was repeated twice with Tris-buffer and two more times with pure water. The final pellets were resuspended in water (1 mL) and equally distributed in 20 separate Eppendorf® tubes.

Synthesis of gold nanoparticles

To ultrapure water (42.5 mL) was added 0.2 M NaOH (1.5 mL) followed by aqueous 0.8 % THPC (1 mL). After 2 min of stirring, aqueous 0.01 M $HAuCl_4$ (5 mL) was added and the mixture turned brown-orange within a few seconds.

Assembly of gold nanoparticles

Freshly prepared gold nanoparticles (AuNPs, 1 mL of the 1 mM colloid suspension described above) were added to each tube containing the multi-layer assembly and the mixture was left at RT for 4 h with 1 min vortex-stirring every 30 min. The suspension was then centrifuged (3000 ×*g*, 5 min) and the nearly colorless supernatant was discarded and replaced with fresh gold colloid suspension (1 mL). The same process was repeated two more times to ensure optimal loading of the tubes with AuNPs. The obtained pellets were washed by 3 consecutive centrifugation-redispersion cycles in water. The 20 pellets were combined and redispersed in water (4 mL) to yield the AuCNTs suspension.

Physical characterization methods

*Inductively coupled plasma mass spectrometry (*ICP-MS*)*

Samples were mineralized at RT for 16 h using *aqua regia*. Subsequently, they were diluted 1000 times by ultrapure water, then 100 times by 2 % HCl and injected via a peristaltic pump equipped with Tygon tubing at 100 $\mu L \cdot min^{-1}$ flow rate. Nebulisation of samples was performed by means of a microconcentric nebulizer. A 7700x ICP-MS (Agilent) was used as elemental detector. ICP conditions were the following: nebulisation gas flow rate: 1 $L \cdot min^{-1}$, dilution gas flow rate: 0.1 $L \cdot min^{-1}$, plasma gas flow rate: 15 $L \cdot min^{-1}$, auxiliary gas flow rate: 1 $L \cdot min^{-1}$. Plasma power was set to 1550 W. Other parameters were adjusted to both maximize the analyte signal and minimize oxide and doubly charged ions formation. Quantification of gold was performed at m/z = 197 using external standards. Between analyses, the system was rinsed for 3 min with 2 % HCl and a blank was injected to control the absence of any memory effect.

X-ray photoelectron spectroscopy (XPS)

An aliquot of the AuCNTs suspension was filtered through a polypropylene membrane which was then dried under vacuum overnight. XPS spectra were acquired on a VG ESCALAB 210 spectrometer.

Transmission electron microscopy (TEM)

Electron microscopy observations were carried out on a Philips CM12 microscope operated at 100 kV.

Electrochemical measurements

The electrochemical analysis of the AuCNTs nanohybrid was carried out using a SP-300 bipotensiostat (Bio-Logic). A speed control unit MSR from Pine Instruments was also used. A three electrode system was used consisting of modified glassy carbon (GC) electrode, Ti wire and an Ag/AgCl/3 M KCl electrode (abbreviated as Ag/AgCl), which acted as the working electrode, counter electrode and reference electrode, respectively. The change of scale *vs.* RHE was done according to Eq. (1):

$$E(V \textit{ vs. } RHE) = E(V \textit{ vs. } Ref.) + E(V \text{ of } Ref. \textit{ vs. } NHE) + 0.059 \times pH \quad (1)$$

Where E(V of Ref. *vs.* NHE)=0.205 V and pH is the pH of the electrolyte used for the experiments and NHE is the Normal Hydrogen Electrode defined by $a_{H+} = 1$ and $a_{H2} = 1$.

AuCNTs nanohybrid-modified GC electrodes were prepared by dropping various volumes (3, 5, 10, 15 and 20 µL) of the sonicated aqueous suspension of AuCNTs nanohybrid onto the surface of a pre-polishied GC disk (0.196 cm^2) of a rotating ring-disk electrode, followed by dropping 5 µL of Nafion solution in ethanol (0.05 wt. %) as a binder before drying under air environment.

Prior to O_2 reduction measurements, the AuCNTs nanohybrid-based electrodes were electrochemically pre-treated and characterized by cyclic voltammetry (CV) in N_2-saturated 0.5 M H_2SO_4 by scanning the potential for 15 cycles between −0.3 and 1.5 V *vs.* Ag/AgCl (-0.077 to 1.723 V *vs.* RHE) at a scan rate of 100 $mV \cdot s^{-1}$.

The catalytic activity of the AuCNTs nanohybrid towards the ORR was tested in a series of rotating disk electrode (RDE), rotating-ring disk electrode (RRDE) and CV measurements under acidic (0.5 M H_2SO_4) and alkaline (0.1 M KOH) conditions. The electrolyte solution was purged with either O_2 or N_2 for 15 min prior to each measurement and a flow of gas was maintained over the electrolyte during the experiments to maintain constant atmosphere. A 10 $mV \cdot s^{-1}$ scan rate was applied for the RDE and RRDE studies. The disk measured current was corrected by subtracting the background current measured in the N_2-saturated solution. Stability experiments were carried out for AuCNT nanohybrid using chronoamperometry with the electrode rotation rate fixed at 1500 rpm (E = 0.6 V *vs.* RHE) in O_2-saturated 0.1 M KOH.

For the 0.5 M H_2SO_4 electrolyte solution, RDE measurements were performed in the applied potential range from +0.4 to −0.3 V *vs.* Ag/AgCl (+0.623 to −0.077 V *vs.* RHE). The cathodic potential was limited to −0.3 V *vs.* Ag/AgCl (−0.077 V *vs.* RHE) to avoid contamination with the H_2 evolution

current or the reduction current for the carbon support. Polarization curves were recorded with various rotation rates (ω) of 500, 1000, 1500, and 2000 rpm. The ring potential in RRDE measurements was kept at 1 V *vs.* Ag/AgCl (1.223 V *vs.* RHE). For 0.1 M KOH electrolyte, the disk potential was scanned from +0.2 to −1 V *vs.* Ag/AgCl (+1.185 to −0.015 V *vs.* RHE), while the ring potential was kept at 0.45 V *vs.* Ag/AgCl (1.435 V *vs.* RHE).

Stability measurements in alkaline media

The stability of AuCNT nanohybrid catalyst in alkaline medium was evaluated by chrono-amperometry at a constant voltage of 0.6 V *vs.* RHE and the electrode rotation rate at 1500 rpm (Fig. S5).

Electrocatalytic activity of the AuCNTs nanohybrid for O_2 reduction in acidic media

In 0.5 M H_2SO_4, oxygen is reduced from 0.2 V *vs.* Ag/AgCl (0.423 V *vs*. RHE) at the AuCNT nanohybrid electrode, which corresponds to 800 mV overpotential. The catalytic activity is under the control of O_2 diffusion (Fig. S2a) and linearly increases with the loading of AuCNTs nanohybrid (Fig. S2b). Rotating ring-disk electrode (RRDE) measurements (Fig. S2b) indicate an overall 4-electron reduction of O_2 to water for potentials more cathodic than 0.1 V *vs*. Ag/AgCl (0.323 V *vs.* RHE). Indeed very low amount of hydrogen peroxide (H_2O_2) are detected during O_2 reduction (Fig. S2c). Tafel slopes calculated from the curves shown in Fig. S2b are close to 100 mV·dec^{-1} (Fig. S3), which, together with the high overpotential requirement,[3,4] suggests that hydrogen peroxide production is the rate-limiting step in ORR under acidic conditions. In order to gain more insights in the catalytic ORR mechanism, we recorded CVs in the presence of H_2O_2. Reduction of H_2O_2 on the AuCNTs nanohybrid electrode occurs with onset potential of 0.2 V *vs.* Ag/AgCl (0.423 V *vs*. RHE, trace b' in Fig. S4), although the catalytic plateau is not reached before −0.16 V *vs.* Ag/AgCl (0.063 V *vs*. RHE). When both O_2 and H_2O_2 are present in the solution, the reduction processes of both substrates occur concomitantly as shown by the increase of the wave at +65 mV (0.288 V *vs*. RHE)in trace b compared to trace a in Fig. S4.

We conclude that the overall 4 e-reduction of O_2 to H_2O catalyzed by AuCNTs nanohybrid under acidic condition is a two-step ($2e^- + 2\ e^-$) process. We note that bulk Au electrodes only mediate the $2e^-$ reduction of O_2 to H_2O_2 without further reduction of H_2O_2 to water,[5,6] and that 4 e^- reduction process is quite rare[7,8] in Au NPs-catalyzed electrocatalytic O_2 reduction in acidic media.[9-11]

Supplementary Figures

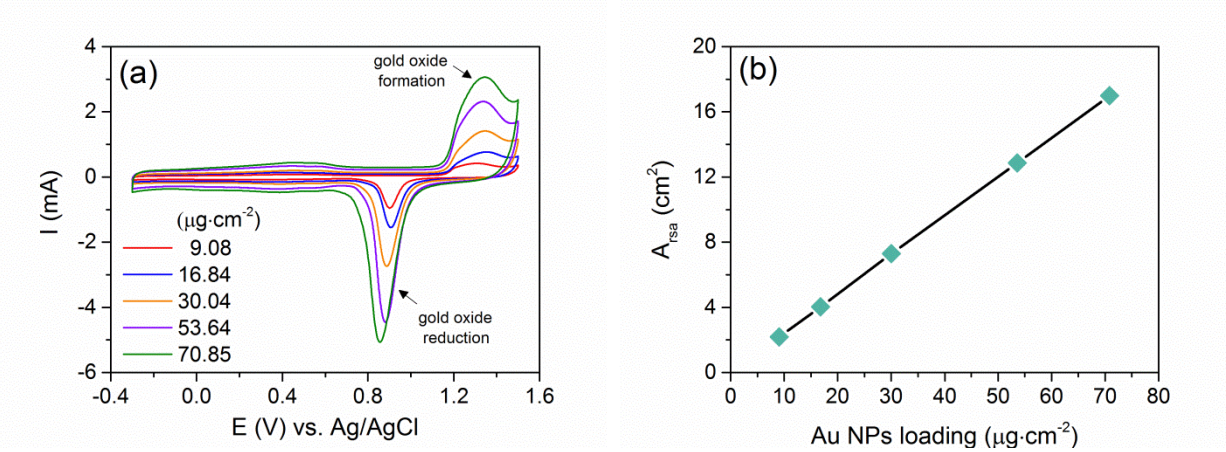

Figure S1 (a). Cyclic voltammograms for AuCNTs nanohybrid drop-cast onto GC electrode (5 mm diameter) in N_2-saturated 0.5 M H_2SO_4 for different Au-loadings (in μg·cm^{-2}) (scan rate: 100 mV·s^{-1}); (b). Variation of the real surface area of the electrode with the AuNPs loading.

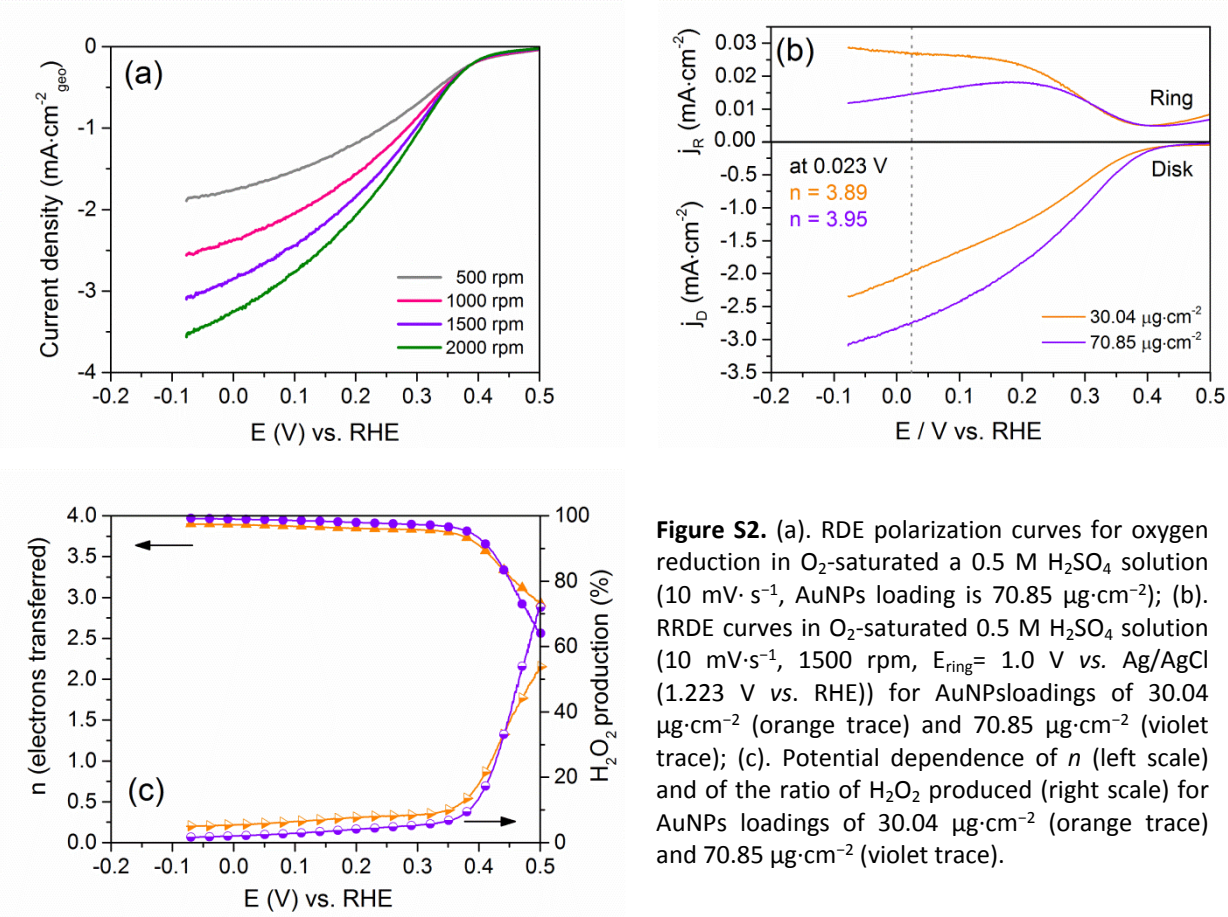

Figure S2. (a). RDE polarization curves for oxygen reduction in O_2-saturated a 0.5 M H_2SO_4 solution (10 mV· s^{-1}, AuNPs loading is 70.85 μg·cm^{-2}); (b). RRDE curves in O_2-saturated 0.5 M H_2SO_4 solution (10 mV·s^{-1}, 1500 rpm, E_{ring}= 1.0 V *vs.* Ag/AgCl (1.223 V *vs.* RHE)) for AuNPsloadings of 30.04 μg·cm^{-2} (orange trace) and 70.85 μg·cm^{-2} (violet trace); (c). Potential dependence of *n* (left scale) and of the ratio of H_2O_2 produced (right scale) for AuNPs loadings of 30.04 μg·cm^{-2} (orange trace) and 70.85 μg·cm^{-2} (violet trace).

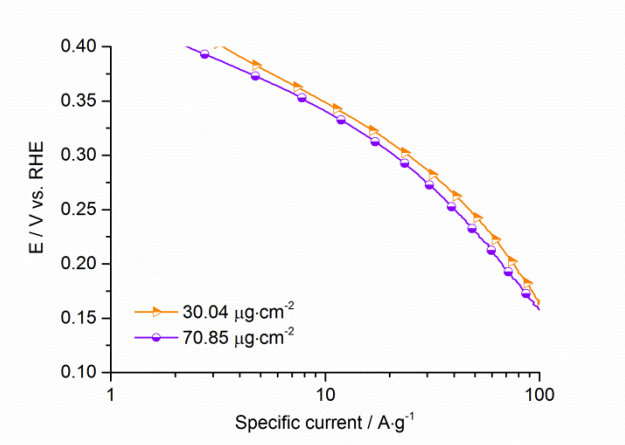

Figure S3. Tafel plots for oxygen reduction on AuCNTs nanohybrid (deriverd from curves shown in Figure S2b, disk) AuNPs loading is 30.04 μg·cm^{-2} (orange) and 70.85 μg·cm^{-2} (violet).

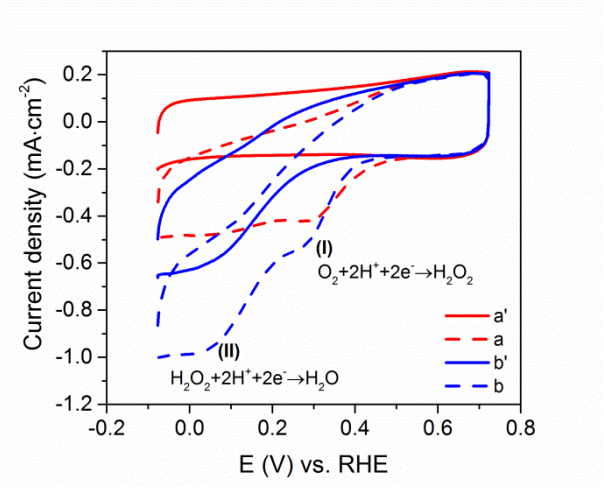

Figure S4. Cyclic voltammograms on AuCNTs nanohybrid in 0.5 M H_2SO_4 solution saturated with N_2 (a', b'), or O_2 (a, b), in the absence (a, a') and the presence (b, b') of H_2O_2 (potential scan rate: 20 mV·s^{-1}, AuNPs loading: 30.04 μg·cm^{-2}, 2.8 mM H_2O_2).

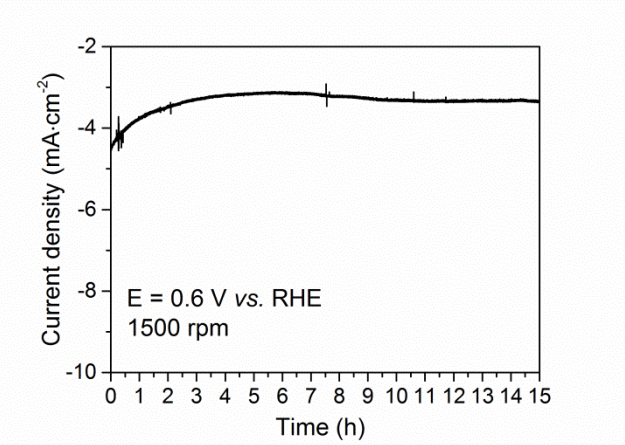

Figure S5 (a). Chronoamperometric curve of the ORR on AuCNT nanohybrid in O_2-saturated 0.1 M KOH solution at E = 0.6 V *vs.* RHE and 1500 rpm (AuNp loading is 70.85 μg·cm^{-2}).

Table S1. Characteristics of Au NPs/CNTs catalyst with different Au NPs loadings

Vol. suspension onto GC (μL)	[a] $m_{Au\ NPs}$ (μg)	[b] Au NPs loading (μg·cm^{-2})	[c] Au NPs loading (μg·cm^{-2})	[d] Q_{neg} (mC)	[e] A_{rsa} (cm^2)	[f] S (cm^2·μg^{-1})
3	2.01	10.25	9.08	0.872	2.18	122.5
5	3.35	17.09	16.84	1.617	4.04	122.4
10	6.70	34.17	30.04	2.919	7.29	123.8
15	10.04	51.26	53.64	5.150	12.87	122.4
20	13.40	68.35	70.85	6.803	17	122.4

[a] As calculated theoretically from the mass of the catalyst applied onto the GC.

[b] As calculated from the dropped volumes of the aqueous suspension of Au NP/CNTs onto GC (Au NPs loading=$[C_M \times V \times A_{Au}]/A_{gsa}$; where C_M=3.4×10^{-3} mol·L^{-1}, V is the volume of the aqueous suspension of Au NP/CNTs catalyst dropped onto GC, A_{Au}=197 g·mol^{-1}, A_{gsa} is geometric surface area)

[c] As estimated from the stable cyclic voltammograms by charge integration under the oxide reduction peak (Au NPs loading= $[Q_{neg}/F \times A_{gsa}] \times A_{Au}$; F- Faraday's constant, A_{gsa}- geometric surface area; A_{gsa} is geometric surface area; A_{Au}=197 g·mol^{-1})

[d] Q_{neg} is the charge under the gold oxide reduction peak

[e] A_{rsa} is the real surface area (as estimated from the charge consumed by the reduction process of the surface oxide monolayer (the peak at *ca* 900 mV in Fig. S1a and using a reported value of 400 μC·cm^{-2}, [12, 13] though precise determination is generally difficult $A_{rsa}=Q_{neg}(mC)/0.400(mC \cdot cm^{-2})$)

[f] S is the specific surface area ($S=(A_{rsa}/WA_{gsa}) \times 100$, W(in μg·cm^{-2}) is the amount of Au NPs loading from [b])

References

1. P. Chen, H. B. Zhang, G. D. Lin, Q. Hong and K. R. Tsai, *Carbon* **1997**, *35*, 1495-1501.

2. J. John, E. Gravel, A. Hagege, H. Y. Li, T. Gacoin and E. Doris, *Angew. Chem. Int. Ed.*, 2011, **50**, 7533.

3. N. Ohta, K. Nomura and I. Yagi, *J. Phys. Chem. C*, 2012, **116**, 14390.

4. P. Quaino, N. B. Luque, R. Nazmutdinov, E. Santos and W. Schmickler, *Angew. Chem.-Int. Ed.*, 2012, **51**, 12997.

5. A. Sarapuu, K. Tammeveski, T. T. Tenno, V. Sammelselg, K. Kontturi and D. J. Schiffrin, *Electrochem. Commun.*, 2001, **3**, 446.

6. M. S. El-Deab and T. Ohsaka, *Electrochem. Commun.*, 2002, **4**, 288.

7. Y. S. Kim, A. Cha, J. Y. Shin, H. J. Jeon, J. H. Shim, C. Lee and S.-g. Lee, *Chem. Commun.*, 2012, **48**, 8940.

8. R. Zeis, T. Lei, K. Sieradzki, J. Snyder and J. Erlebacher, *J. Catal.*, 2008, **253**, 132.

9. N. Alexeyeva and K. Tammeveski, *Anal. Chim. Acta*, 2008, **618**, 140.

10. N. Alexeyeva, L. Matisen, A. Saar, P. Laaksonen, K. Kontturi and K. Tammeveski, *J. Electroanal. Chem.*, 2010, **642**, 6.

11. M. Bron, *J. Electroanal. Chem.*, 2008, **624**, 64.

12. S. Trasatti and O.A. Petrii, *Pure Appl. Chem*., 1991, **63**, 711.

13. H.A. Kozlowska, B.E. Conway, A. Hamelin and L. Stoicoviciu, *J. Electroanal. Chem.*, 1987, 429.